Onset and Demise of the Southeast Asia Rainy Season

Alice Brennan[1,2], V. Misra[1, 2] , Joanna Rodgers[1, 2], & C. B. Jayasankar[1]

[1]Center for Ocean-Atmospheric Prediction Studies, Florida State University, Tallahassee, Florida, USA

[2]Department of Earth, Ocean and Atmospheric Science, Florida State University, Tallahassee, Florida, USA

Abstract

This study uses an objective definition for the onset and demise date for the seasonal evolution of the rainy season over the Southeast Asia (SEA) region. The onset or the demise date is defined as the first or the last date of the year when the daily rain rate exceeds the annual mean climatological rainfall. This gives rise to a varying length of the season that has a significant impact on the seasonal rainfall. It is observed that the interannual variability of the seasonal rainfall is significantly affected by the variations of the onset and demise dates. But the influence of the onset and demise date appears to be independent of each other. Using the Integrated Multi-Satellite Retrievals for Global Precipitation Mission version 6 (IMERG) rainfall analysis available on 0.1°grid we have analyzed the variations of the rainy season over SEA. We generate an ensemble of 1001 members by slightly perturbing the original timeseries to account for uncertainties in the rainfall analyses. This also ensures that the diagnoses of the onset/demise dates are not sensitive to sporadic synoptic/mesoscale rain events that may be unconnected to the seasonal evolution of rainfall in SEA. Using these ensemble of 1000 members per season, we find that we can provide reliable probabilistic outlook of the forthcoming rainy season over the SEA region.

Introduction

The Southeast Asia (SEA) region is located in the Northern Hemisphere between the Indian Ocean and the Pacific Ocean. With a population of over 680,000,000 million people, this area is a dominant force in agriculture, culture, industry, and of course, meteorological phenomena. The region is situated between two oceans and influenced by a multitude of teleconnections, such as the Indian Ocean Dipole (IOD), the Madden Julian Oscillation (MJO), the El Nino Southern Oscillation (ENSO), etc. One of the most notable meteorological events to occur in this region is the Asian monsoon, which can be separated into two categories: the Indian summer monsoon and the East Asian summer monsoon (Misra and DiNapoli 2013). This study is specifically going to target the East Asian monsoonal region, including Myanmar, Thailand, Laos, Cambodia, and Vietnam. Four values are determined for every day from 2001-2022 in the region: onset start date, demise end date, length of rainy season, and rain totals. Additionally, correlation values between the El Nino-Southern Oscillation (ENSO) the calculated parameters above, to see how the ENSO pattern affects the monsoon and dry season (Hariadi 2022).

Datasets & Methodology

We use NASA's IMERG 12h latency, gridded, daily, global, precipitation (Huffman et al. 2019) data available from 2000 to the present at 0.1° grid resolution. The methodology adopted in this study to diagnose the onset and demise of the wet season has been widely used for many of the tropical regions that show strong seasonality of rainfall (Liebmann and Marengo 2001; Misra and DiNapoli 2014; Dunning et al. 2016; Uehling and Misra 2020). Essentially, this methodology diagnoses the first and the last day of the year when the daily rain rate exceeds the corresponding climatological annual mean rainfall as the onset and the demise of the wet season. This methodology is effective only where there is a strong seasonality of rainfall. The objective definition of onset and demise of the rainy season follows from Noska and Misra (2016). We define the onset and demise based on the inflection points of the cumulative daily anomaly of rainfall given by:

$$P'_n(k) = \sum_{m=1}^{k}\left[P_n(m) - \overline{\overline{P}}\right] -------------(1)$$

where, $P_n(m)$ is the area average daily rainfall for day m of year n averaged over a given region, $\overline{\overline{P}}$ is the corresponding annual mean rainfall climatology. The minimum (maximum) in $P'_n(k)$ is defined as onset (demise) date of the RSPF (Fig. 1).

Additionally, given the uncertainty of observations, analysis techniques, and discretization of the rainfall data, Misra et al. (2023) introduced perturbations of the timeseries to obtain a robust ensemble of onset and demise dates from a given daily rainfall. Obtaining such an ensemble of onset/demise dates also precludes their diagnosis from excessive bearing of isolated synoptic or sub-synoptic rain bearing systems, which may be unconnected to the large-scale seasonality of the rainfall. Following Misra et al. (2023), the perturbations are generated by shuffling the original daily timeseries on the timescale of 6 days (representing synoptic scales) with rain rates of some randomly chosen days being replaced by rain rates occurring within the sequence of 3 days of the chosen date. We generate 1000 perturbed timeseries.

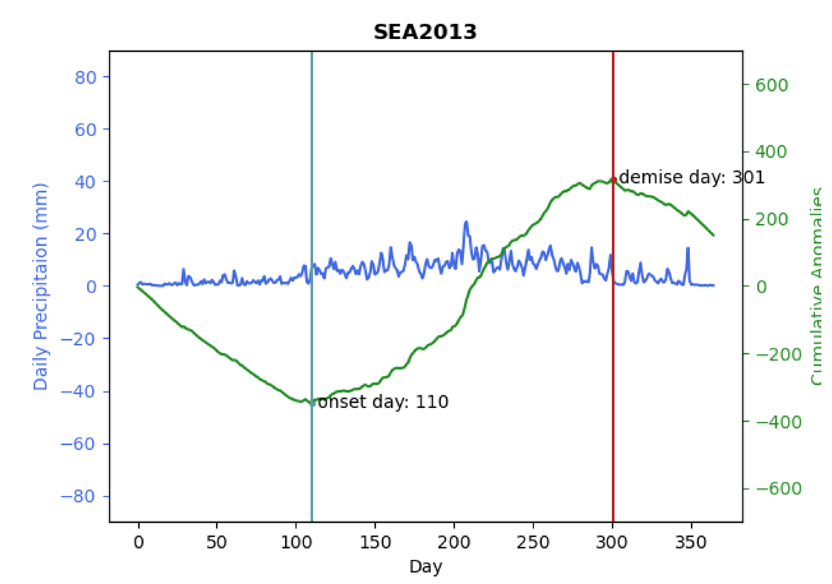

Figure 1: A schematic illustration of the time series of daily rainfall (blue bars; mm day^{-1}) and its corresponding cumulative daily anomaly (P' in equation 1; green line; mm) over a the entire SEA region for the year 2013. The onset (Julian Day: 110 (April 20)) and demise (Julian Day: 301 (October 28)) dates of the rainy season are indicated in the figure.

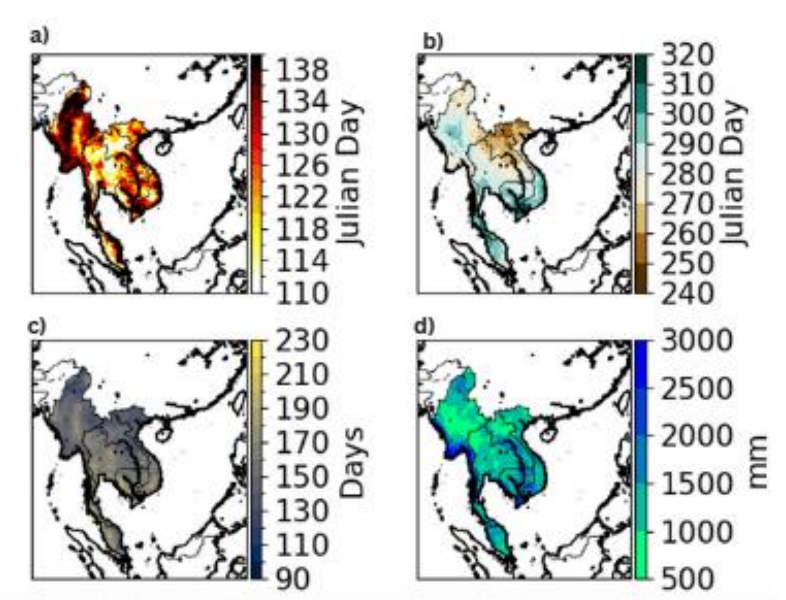

Figure 2: The climatological median (a) onset date, (b) demise date, (c) seasonal length, and (d) seasonal rain from IMERG.

Results

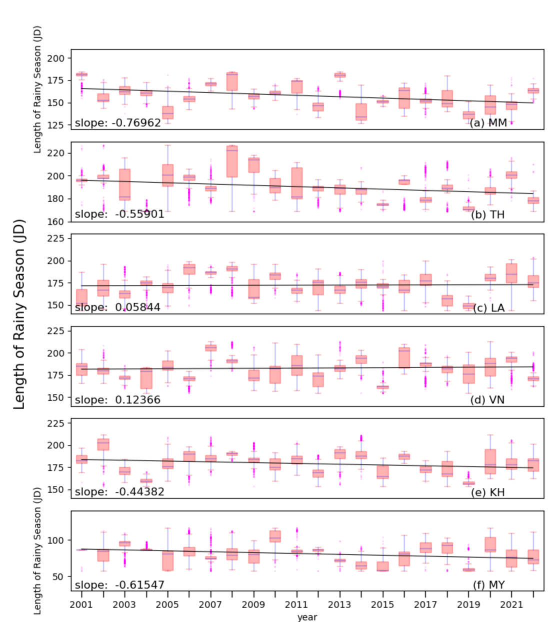

Figure 3: Box and whisker plot of the length of the rainy season for a) Myanmar, b) Thailand, c) Laos, d) Vietnam, e) Cambodia, and f) Malaysian Peninsula. The median value is indicated by the red line (approximately in the middle of the box) with the top and bottom edges of the box representing the 75th and the 25th percentile and the whiskers and dots representing the extreme data points of the ensemble spread and outliers (more than 1.5 times the inter-quartile range), respectively. The least squares fit line (black solid line) through the median value is overlaid with the 95% confidence interval (dotted lines). The slope of the least square fit is also indicated in each panel..

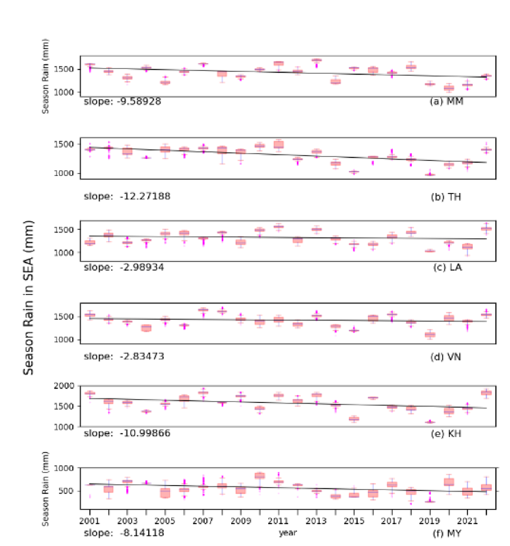

Figure 4: Box and whisker plot of the seasonal rain of the rainy season for a) Myanmar, b) Thailand, c) Laos, d) Vietnam, e) Cambodia, and f) Malaysian Peninsula. The median value is indicated by the red line (approximately in the middle of the box) with the top and bottom edges of the box.

Interannual Variability

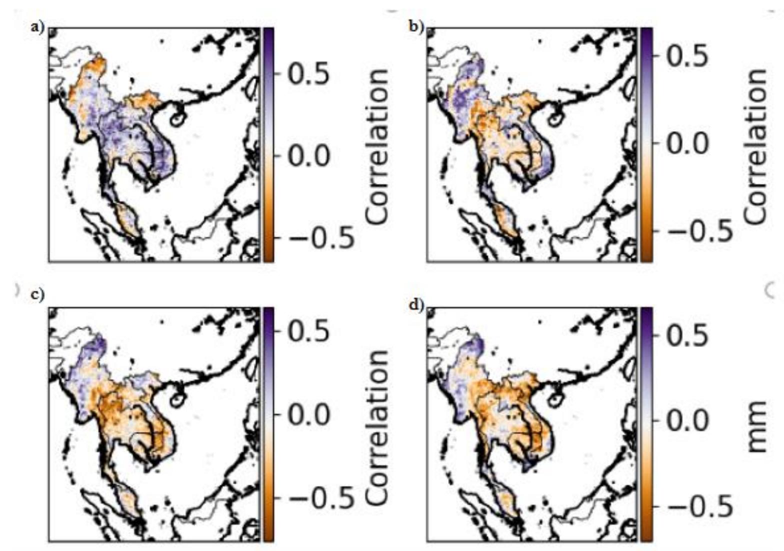

Figure 5: The correlation of preceding DJF Niño3.4 SST index (OISSTv2; Reynolds et al. 2002) with anomalies of (a) onset date, (b) demise date, (c) seasonal length, and (d) seasonal rain of the rainy season.

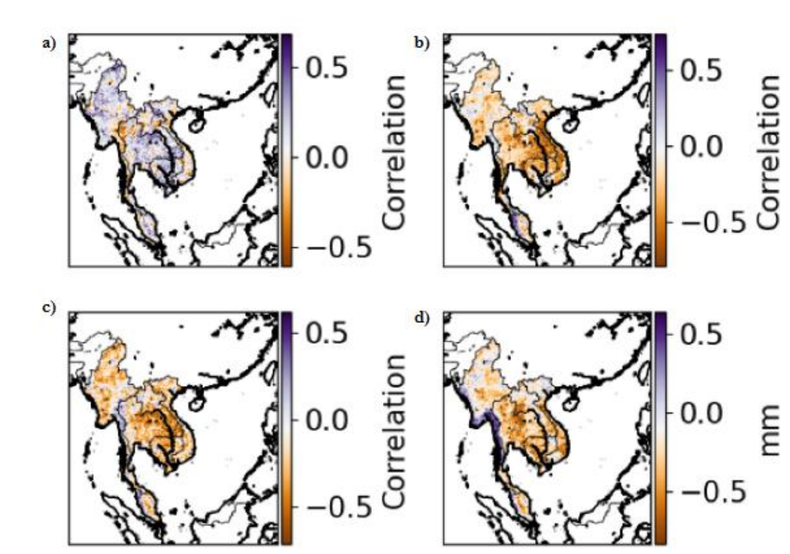

Figure 6: The correlation of concurrent JJA Nino3.4 SST index (OISSTv2; Reynolds et al. 2002) with anomalies of (a) onset date, (b) demise date, (c) seasonal length, and (d) seasonal rain of the rainy season.

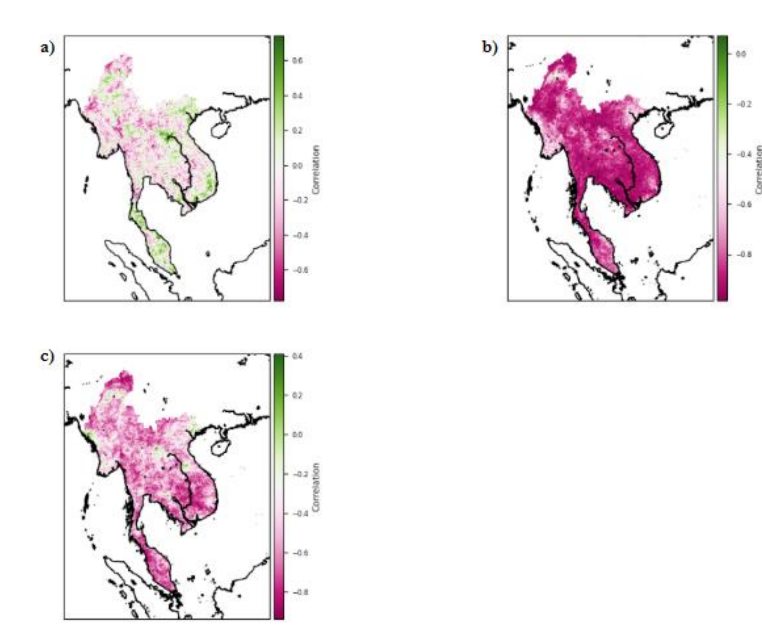

Figure 7: The 95% correlations of the onset date with anomalies of (a) demise date (b) length, and (c) seasonal rain.

(a) Onset and demise dates are insignificantly correlated.
(b) Early/later onset is associated with longer or shorter length of the wet season, respectively.
(c) Early/later onset is associated with wetter or drier rainy season, respectively.

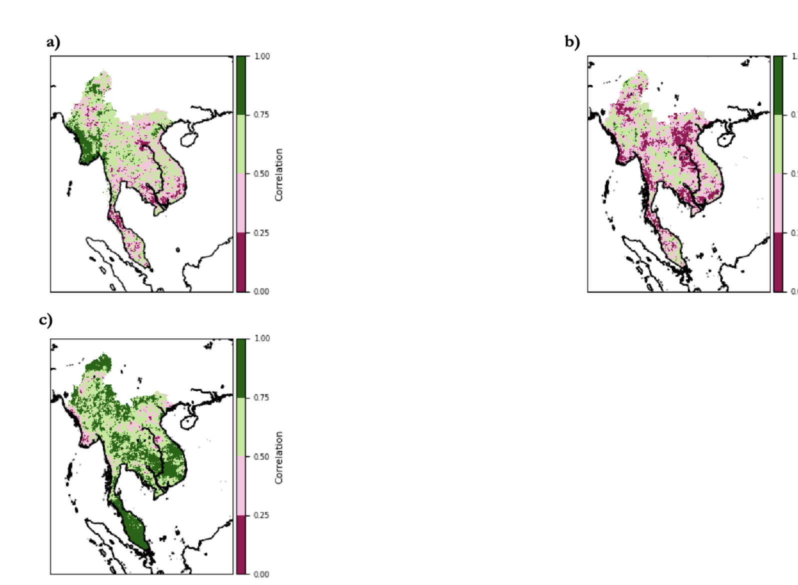

Figure 8: The 95% correlations of the demise date with anomalies of (a) length and (b) seasonal rain of the wet season. (c) The correlations of the seasonal length with corresponding seasonal rainfall anomalies of the wet season.

(a) Early/later demise is associated with shorter or longer length of the wet season, respectively.
(b) Early/later demise is associated with drier or wetter rainy season, respectively.
(c) Longer or shorter seasonal length is associated with wetter or drier rainy season, respectively.

Efficacy of monitoring onset of the wet season

The Relative Operating Characteristic (ROC) curve is a plot between the false alarm rate and the hit rate that measures the probabilistic skill for a binary choice. The Area under the ROC curve (AROC) sums up how well a model can produce scores to discriminate between correct and incorrect choices. The AROC score ranges from 0 to 1, where < 0.5 indicates the skill is as good as random guessing and 1 indicates perfect performance. The following figures show the AROC scores for skill in predicting wetter (and longer) or drier (and shorter) season from monitoring early or late onset of the rainy season.

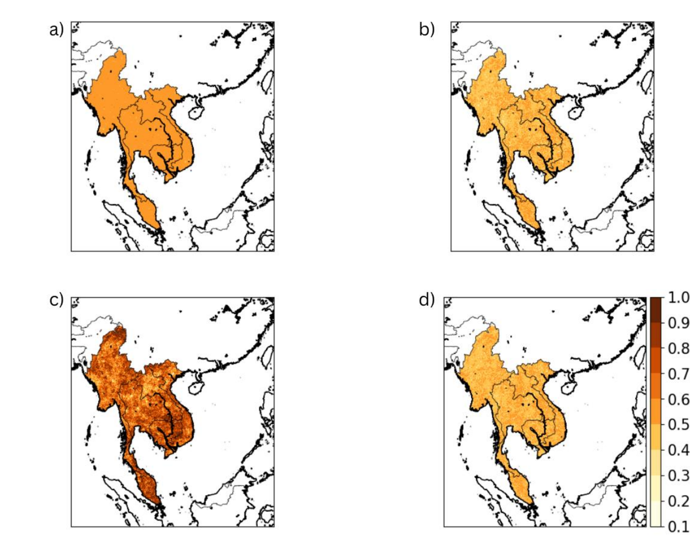

Figure 10: The area under the Relative Operating Characteristic (ROC) curve for the outlook of a) a longer wet season based on early onset, b) a shorter wet season based on later onset, c) a wetter wet season based on early onset and d) drier wet season based on later onset of the wet season.

Conclusions

- There has been a decreasing linear trend in monsoonal season length and rain totals within the past 20 years, most notably in Myanmar and Thailand.
- There is a negative correlation with the onset date and length, along with the onset date and rain totals, indicating that an earlier or a later onset date corresponds to a longer and wetter or a shorter and drier rainy season, respectively.
- Comparatively, there is a positive correlation between the demise dates and the seasonal length and demise dates and rain totals. This indicates that an earlier or later demise results in a shorter and drier or longer and wetter rainy season, respectively.
- The large-scale teleconnections of the southeast Asian monsoon with ENSO are relatively weaker than the internal variations diagnosed and summarized in the earlier two bullet points.
- Therefore, monitoring the variations of the onset date of the Southeast Asian summer monsoon could provide a more reliable outlook of the forthcoming season.

References

Dunning, C. M., E. C. L. Black, and R. P. Allan, 2016: The onset and cessation of seasonal rainfall over Africa. *J. Geophys. Res. Atmos.*, **121**, 11, pp. 405– 11,424, 10.1002/2016JD025428.

Hariadi M. H., and Coauthors, 2022. Evaluation of extreme precipitation over Southeast Asia in the Coupled Model Intercomparison Project Phase 5 regional climate model results and HighResMIP global climate models. Royal Meteorological Society, **43**, 3, https://doi.org/10.1002/joc.7938

Forster, P., T. and Coauthors, 2021: The Earth's Energy Budget, Climate Feedbacks, and Climate Sensitivity. In *Climate Change 2021: The Physical Science Basis. Contribution of Working Group I to the Sixth Assessment Report of the Intergovernmental Panel on Climate Change* **6,** 7, pp. 923–1054, 10.1017/9781009157896.009.

Liebmann, B., and J. Marengo, 2001: Interannual Variability of the Rainy Season and Rainfall in the Brazilian Amazon Basin. *J. Climate*, **14**, pp. 4308–4318, https://doi.org/10.1175/1520-0442(2001)014<4308:IVOTRS>2.0.CO;2.

Misra, V., and S. DiNapoli, 2014: The variability of the Southeast Asian summer monsoon. Int. J. Climatol., **34(3)**, 893-901.

Misra, V., S. Dixit, and C. B. Jayasankar, 2023: The Regional Diagnosis of Onset and Demise of the Rainy Season over Tropical and Subtropical Australia Earth Interactions, Bull. Amer. Meteor. Soc., **27,** 1, https://doi.org/10.1175/EI-D-22-0026.1.

Narotsky, C. D. and V. Misra 2022: The Seasonal Predictability of the Wet Season over Peninsular Florida Int. J. Climatol., **42,** 6, https://doi.org/10.1002/joc.7423.

Noska, R. and V. Misra 2016: Characterizing the onset and demise of the Indian summer monsoon. Geophysical Research Letters, **43**, 9, 4547-4554.**https://doi.org/10.1002/2016GL068409**

Uehling, J. and V. Misra, 2020: Characterizing the seasonal cycle of the Northern Australian rainy season. J. Climate, **33**, 8957-8973.

Vera, C., W. Higgins, J. Amador, T. Ambrizzi, R. Garreaud, D. Gochis, D. Gutzler, and coauthors, 2006: Toward a unified view of the American monsoon systems. J. Climate, **19,** 20, p. 4977-5000, https://doi.org/10.1175/JCLI3896.1.

Acknowledgement

The authors gratefully acknowledge the support given by NASA GRANT 80NSSC22K0595. The IMERG dataset was provided by the NASA/Goddard Space Flight Center.